155
8-20-79

DR 3016

LA-7907-PR

Progress Report

MASTER

Geostatistics Project of the National Uranium Resource Evaluation Program

October 1978—March 1979

University of California

LOS ALAMOS SCIENTIFIC LABORATORY
Post Office Box 1663 Los Alamos, New Mexico 87545

GEOSTATISTICS PROJECT OF THE NATIONAL URANIUM RESOURCE EVALUATION PROGRAM
October 1978 -- March 1979

by

R. J. Beckman, T. R. Bement, K. Campbell, J. S. Howell, G. W. Wecksung, and D. E. Whiteman

ABSTRACT

During the period covered by this report, research was concentrated on multivariate approaches to the analysis of aerial radiometric data. Two aspects of principal components analysis were the subjects of two publications. The procedures recommended for linear discriminant analysis were revised. Progress was made in overlaying LANDSAT data with aerial radiometric data from the Lubbock quadrangle.

Some preliminary results from principal components analysis of the Wind River data were obtained.

I. INTRODUCTION

This report outlines the activities and progress of the Los Alamos Scientific Laboratory (LASL) on the Geostatistics project during the first half of FY1979. The Geostatistics project is part of the National Uranium Resource Evaluation (NURE) program sponsored by the US Department of Energy (DOE) Grand Junction, Colorado, office. The NURE program is designed to assess the potential uranium resources throughout the conterminous United States and Alaska. The Geostatistics project at LASL, in close cooperation with the Grand Junction Office of DOE, applies statistical methods to the analysis of data collected by airborne instrumentation. A close statistical consulting relationship is maintained with the DOE Grand Junction office and the Bendix Field Engineering Corporation (BFEC) in Grand Junction to handle a broad range of problems related to the NURE.

During the period covered by this report, research was concentrated on various multivariate approaches to the analysis of aerial radiometric data,

including principal components analysis, linear discriminant analysis and the augmentation of aerial radiometric data by data from other sources (specifically LANDSAT.) Principal components as a technique for locating outliers was included in a paper presented in October,[1] and another aspect of principal components analysis was developed in detail in Ref. 2.

Procedures for validating a linear discriminant function calculation were developed. These procedures should be used before extensive classification of observations using such a function is undertaken. On the basis of results obtained using these procedures, a method for linear discriminant analysis proposed earlier was rejected, and a new method is proposed.

The LANDSAT data corresponding to the area covered by the aerial survey in the western part of the Lubbock quadrangle was extracted.

Further work on the ratio bias problem suggests that earlier results may be an artifact.

Programs implementing some earlier univariate techniques (the robust detection of outliers[3] and the determination of segments with maximum variance[4]) were given to the Bendix Field Engineering Corporation in Grand Junction for a further testing and use. Programs for discriminant analysis will be available soon.

Some data from the Wind River and Powder River basins were received. These tapes include no geological information so that most of the techniques explored in the past cannot be applied. However, some displays and some preliminary results using principal components analysis are available.

II. PRINCIPAL COMPONENTS

Principal components analysis as a technique for locating anomalies in the aerial data was discussed in two earlier reports.[5,6] The underlying idea there is that the principal components of the data define a new coordinate system, whose principal axis is aligned with the bulk of the data. Outliers can be expected to show up relative to the axes defined by the second and third components. Figure 1 illustrates this in two dimensions. The anomalous population in this data, although its center is well removed from the center of the main population, is not separated by projection onto either of the original axes (Fig. 1a), nor is it distinguished by extreme values of the ratio Y/X (Fig. 1b). However, projection onto the second axis of the

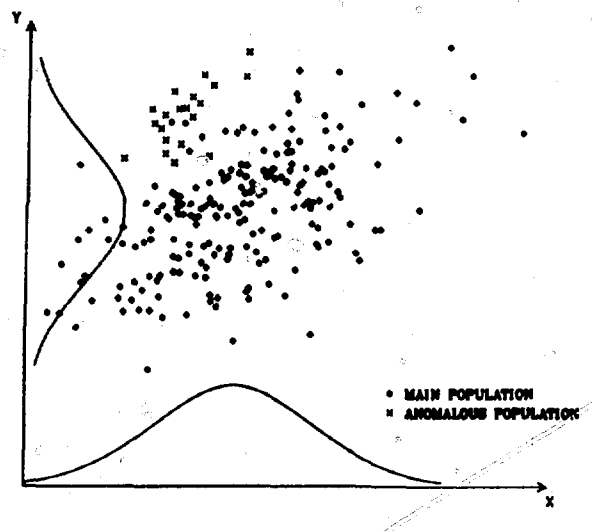

Fig. 1a. Marginal distributions of a mixture of two bivariate normal populations.

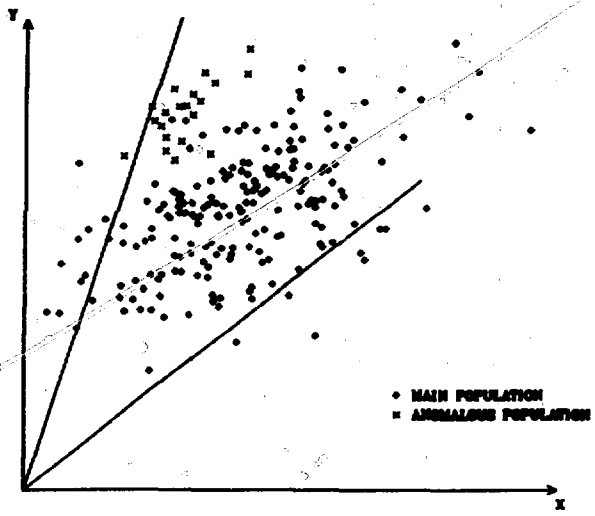

Fig. 1b. Lines of constant ratio superimposed on a mixture of two bivariate normal populations.

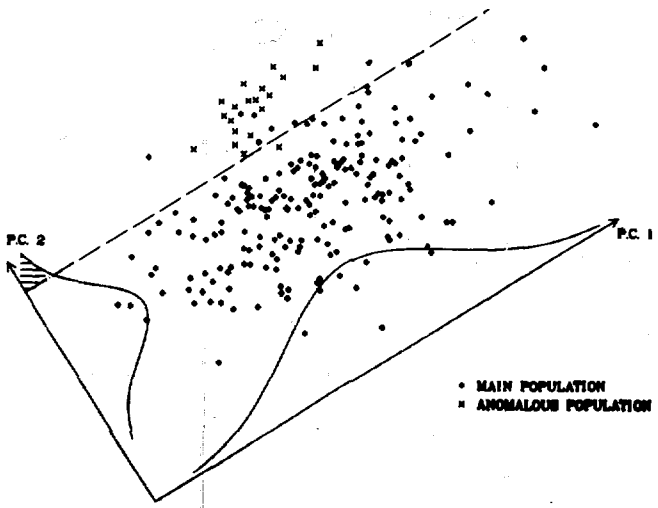

Fig. 1c. Projection of a mixture of two bivariate normal populations on axes determined by the principal components of the data.

data-defined principal coordinate system separates out the anomalous population quite well (Fig. 1c).

The aerial data does not come from a homogeneous population, as in the above example, and in order to obtain interesting results the principal components should be computed within mapped geological types. Perhaps robust techniques should also be used, by analogy with earlier work in outlier detection.[3] These ideas are being pursued. However, in the period covered by this report, some interesting aspects of principal components computed without regard to the mapped geology have been explored. This exploration was significantly aided by the availability of gray-level displays of functions of the aerial data which were developed earlier.[7]

The first principal component of the data is the direction along which the data vary most about their mean vector in the three-dimensional space defined by the observed thallium, bismuth, and potassium counts. It can be expected that a map of this factor (constructed by projecting the three-dimensional data onto the first principal axis and depicting the resulting scalar values by light and dark shades of gray) will reflect the largest source of variability in the data. Because the calculation here has been done without normalizing with respect to geology, the major contribution to the variance will be the underlying geological variation (or more broadly, perhaps, the original depositional environment; see Ref. 1 for details). Figure 2a is a map of the first principal factor for the Lubbock and Plainview, and the most obvious boundaries correspond to known geological discontinuities.

The first principal factor is positively correlated with all of the aerial radiometric bands (Table I), and with total counts. The other principal components can be thought of as "contrasts" among the three bands. For example, the map of the second factor (Fig. 3a) is a gray-level picture of the linear combination

$$p_2 = .188\ \mathrm{Tl} + .922\ \mathrm{Bi} - .338\ \mathrm{K},$$

which is large (light) where there is a large count in the bismuth (and thallium) bands relative to the potassium band, compared to the average relationship among these bands over the whole quadrangle. This might be the result of selective sorting based on the chemical solubility of the parent

TABLE I

Principal Components Using the Covariance Matrix of Reduced Counts, Lubbock and Plainview Quadrangles

	Mean	Covariance Matrix			Principal Components			Correlation of Factors with Original Variables		
	μ	Σ			ϕ_1	ϕ_2	ϕ_3	z_1	z_2	z_3
Y_1 (Tl)	57.0	299.7	267.6	438.1	0.245	0.188	0.951	0.674	0.312	0.669
Y_2 (Bi)	85.6	267.6	901.6	356.9	0.289	0.922	-0.256	0.459	0.882	-0.104
Y_3 (K)	206.3	438.2	256.8	2042.6	0.925	-0.338	-0.172	0.976	-0.215	-0.046
				Variance =	2270.1	825.4	148.4			
				(%) =	(70.0)	(25.4)	(4.6)			

elements, and could indicate areas where uranium has been depleted or concentrated by geological processes. Such conjectures are further explored in Ref. 1.

Because the aerial data (at least in its raw form) is count data, there is a possibility that even the data used in these calculations (which has been corrected for background, altitude, and scattering and considerably smoothed) exhibits some counting type statistics. In particular, the variance of the data may increase in proportion to the mean, causing segments of the data with high average value to exert undue influence on the principal component calculation, which is supposed to reflect variance alone. Therefore the principal component calculation was repeated using the square roots of the thallium, bismuth and potassium observations. (The square root is an approximate "variance stabilizing" transformation for count data.) The results are given in Table II and Figs. 2b, 3b and 4b. Despite the differences between the two tables, it is interesting to note that the differences in the resulting displays are marginal.

A third possible transformation (and a natural one if non-counting variables, such as magnetic field data, are to be included in the analysis) is to standardize the data, subtracting the mean from each observation and dividing by the standard deviation. In the Lubbock-Plainview region this leads to results quite similar to those in Table II.

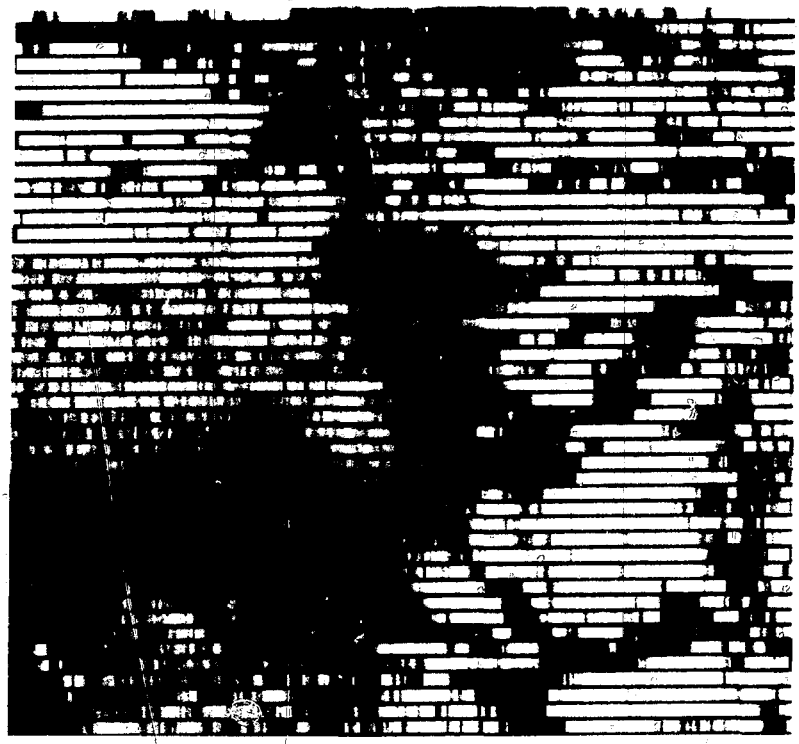

Fig. 2a.

First principal component of the K-U-T data in the Lubbock and Plainview quadrangles--smoothed data.

Fig. 2b.

First principal component of the K-U-T data in the Lubbock and Plainview quadrangles--square roots of smoothed data.

Fig. 3a.

Second principal component of the K-U-T data in the Lubbock and Plainview quadrangles--smoothed data.

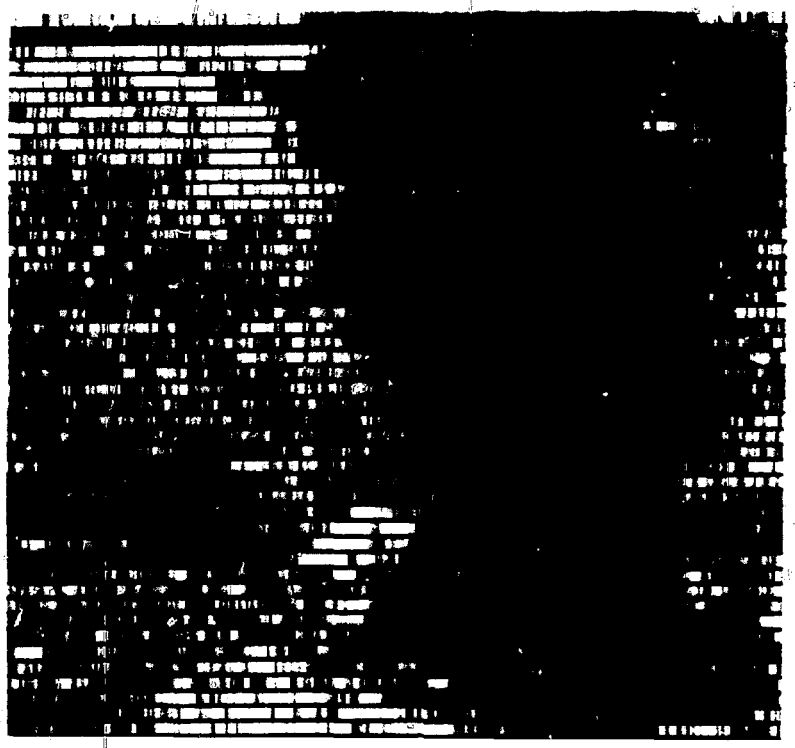

Fig. 3b.

Second principal component of the K-U-T data in the Lubbock and Plainview quadrangles--square roots of smoothed data.

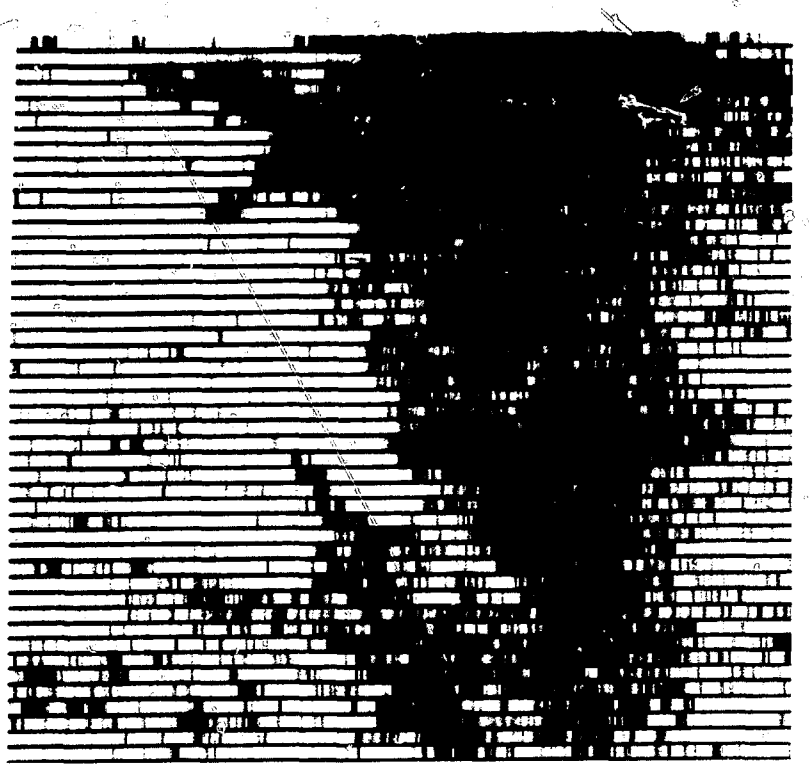

Fig. 4a.

Third principal component of the K-U-T data in the Lubbock and Plainview quadrangles--smoothed data.

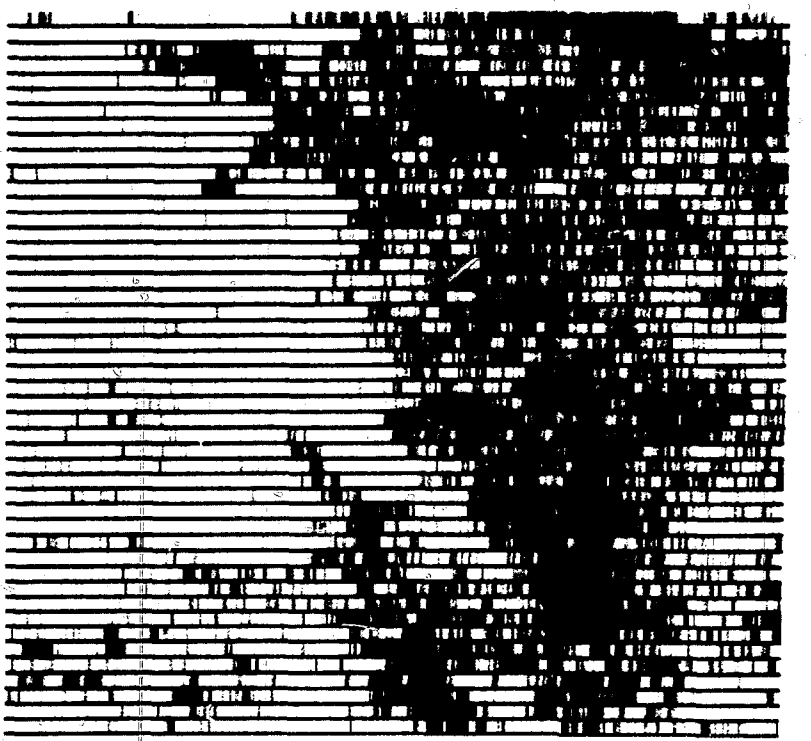

Fig. 4b.

Third principal component of the K-U-T data in the Lubbock and Plainview quadrangles--square roots of smoothed data.

TABLE II

Principal Components Using the Covariance Matrix of the Square Roots of Reduced Counts, Lubbock and Plainview Quadrangles

	Mean	Covariance Matrix			Principal Components			Correlation of Factors with Original Variables		
	ψ	Σ			ϕ_1	ϕ_2	ϕ_3	z_1	z_2	z_3
Y_1 (Tl)	7.46	1.413	1.115	1.135	0.475	0.019	0.880	0.835	0.022	0.550
Y_2 (Bi)	9.11	1.115	2.684	0.836	0.626	-0.710	-0.323	0.798	-0.585	-0.147
Y_3 (K)	14.27	1.135	0.836	2.636	0.618	0.704	-0.349	0.795	0.586	-0.160
				Variance =	4.356	1.824	0.553			
				(%) =	(64.7)	(27.1)	(8.2)			

Tables III and IV show the results of the principal component calculations for the data of the Wind River basin, and Figs. 6, 7 and 8 are the corresponding pictures of the three principal components. Once again very different tables correspond to similar pictures.

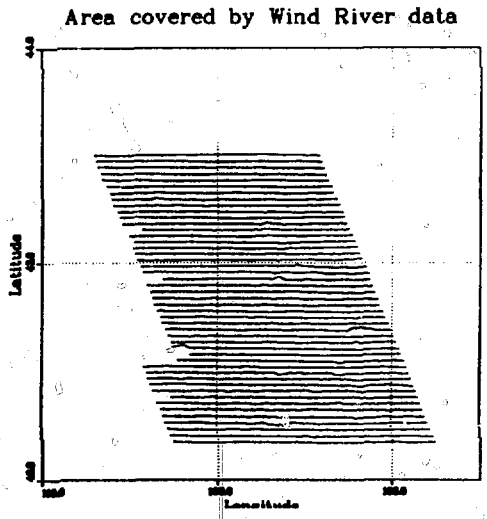

Fig. 5. Area covered by the Wind River maps.

TABLE III

Principal Components Using the Covariance Matrix of the Reduced Counts, Wind River Basin

	Mean	Covariance Matrix			Principal Components			Correlation of Factors with Original Variables		
	μ	Σ			ϕ_1	ϕ_2	ϕ_3	Z_1	Z_2	Z_3
Y_1 (Tl)	171.	8776.	2322.	8386.	.459	.824	.333	.782	.611	.124
Y_2 (Bi)	92.	2322.	1948.	2150.	.126	.311	-.942	.454	.489	-.745
Y_3 (K)	500.	8386.	2150.	20805.	.880	-.474	-.039	.974	-.228	-.009
		Variance =			25487.	4826.	1217.			
		(%)			(80.8)	(15.3)	(3.9)			

TABLE IV

Principal Components Using the Covariance Matrix of the Squares Roots of the Data, Wind River Basin

	Mean	Covariance Matrix			Principal Components			Correlation of Factors with Original Variables		
	μ	Σ			ϕ_1	ϕ_2	ϕ_3	Z_1	Z_2	Z_3
Y_1 (Tl)	12.7	9.233	3.237	6.474	.649	.540	.537	.897	.366	.247
Y_2 (Bi)	9.4	3.237	3.579	2.092	.255	.510	-.821	.568	.556	-.607
Y_3 (K)	22.1	6.474	2.092	11.064	.717	-.670	-.193	.906	-.416	-.081
		Variance =			17.67	4.26	1.96			
		(%)			(74.0)	(17.8)	(8.2)			

The third factor in the Wind River data has a high correlation with bismuth, and the displays in Fig. 8 clearly reveal a problem with the data. Figure 9 is a plot of the bismuth mean as a function of map line number, with the arrows showing the order in which map lines were flown each day (except that line 1 was flown before line 2, not as indicated). This plot quickly suggests that the problem is a time-of-day effect, as the contractors recognized in their final report.[8]

Fig. 6a.

First principal component of the K-U-T data in the Wind River Basin, single record data.

Fig. 6b.

First principal component of the K-U-T data in the Wind River Basin, square roots of single record data.

Fig. 7a.

Second principal component of the K-U-T data in the Wind River Basin, single record data.

Fig. 7b.

Second principal component of the K-U-T data in the Wind River Basin, square roots of single record data.

Fig. 8a.

Third principal component of the K-U-T data in the Wind River Basin, single record data.

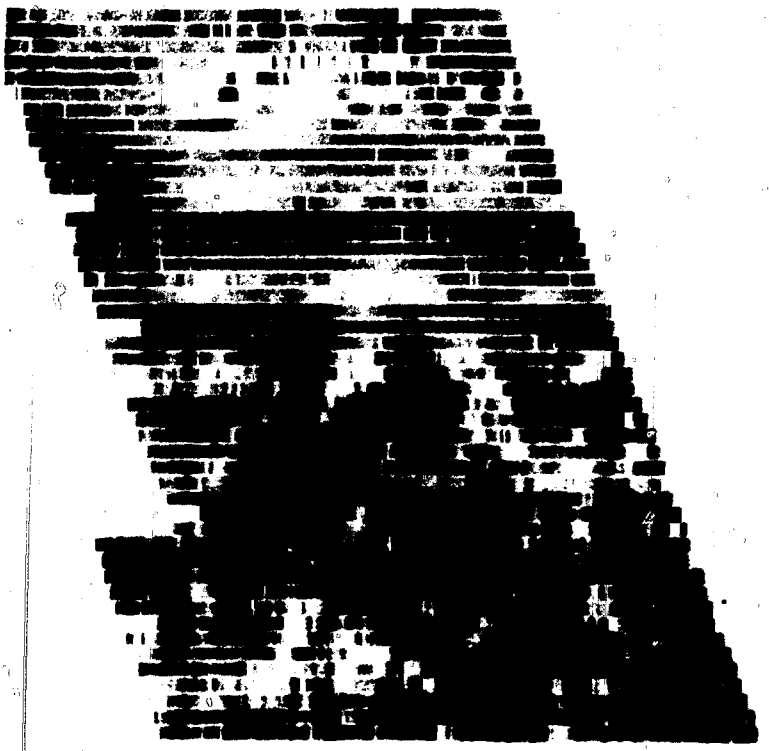

Fig. 8b.

Third principal component of the K-U-T data in the Wind River Basin square roots of single record data.

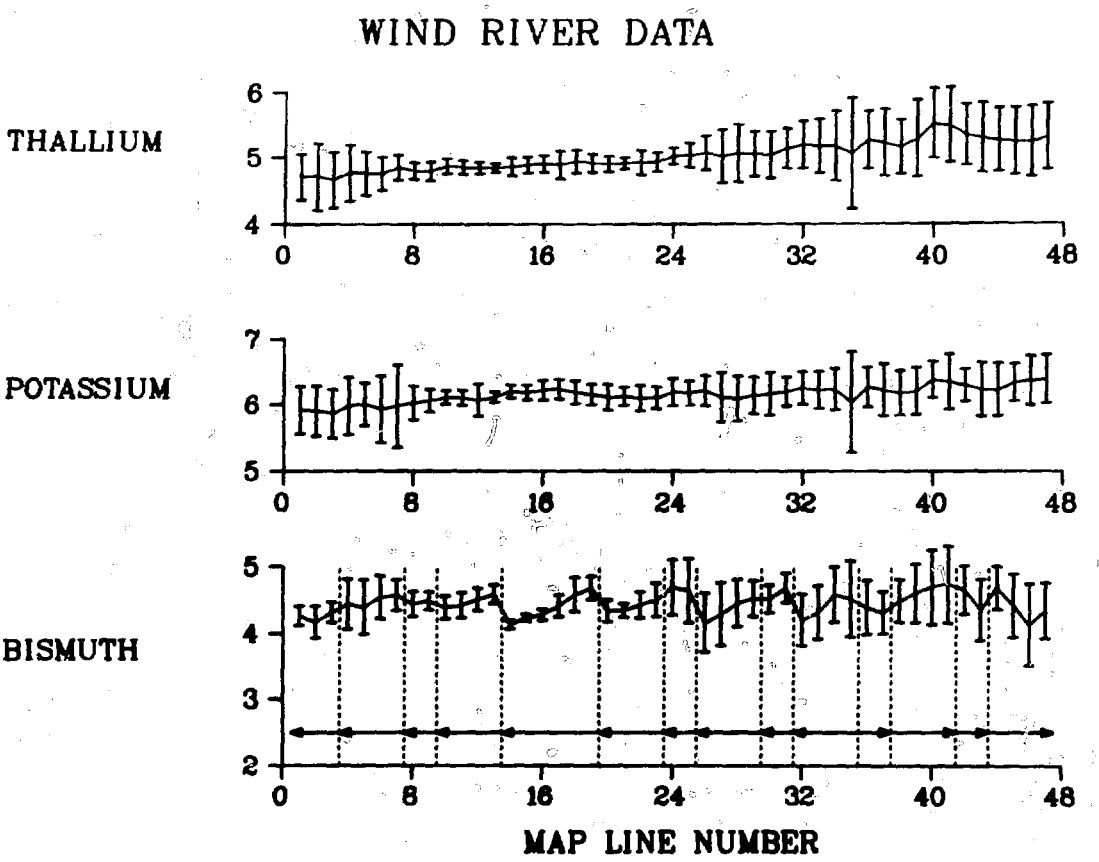

Fig. 9. Average ^{208}Tl, ^{40}K and ^{214}Bi readings as a function of flight line.

III. LINEAR DISCRIMINANT ANALYSIS

Linear discriminant analysis was discussed in two earlier reports.[3,9] It is a technique which leads to a rule for classifying new observations as "favorable" or "unfavorable" indicators of uranium potential, based on the similarity of the new observations to those collected over areas of known mineralization or over areas known to be barren. A "learning set" consisting of several regions in the Lubbock quadrangle (approximately half of which were thought to be favorable on the basis of ground studies) was acquired in the last quarter of FY1978. The linear discriminant studies are based on segments of aerial data 100 observations in length which were flown in the vicinity of these regions.

Earlier work used sample statistics computed from these segments as variables on which to base the computation of the linear discriminant function. The variance of bismuth, the skewness of the distribution of the Bi/Tl ratio, and many other characterizations of the 100-observation samples were computed. A stepwise procedure was used to select a subset of these statistics to maximize the discriminating power of the corresponding linear discriminant function. The statistics chosen did not always correspond to quantities to which geological significance could be attached. More serious, perhaps, is the fact that this procedure performed poorly with respect to the criteria discussed below. Therefore, the following work is based on the direct aerial radiometric measurements (counts in the bismuth, thallium and potassium bands) and their ratios, normalized by mapped geological type.

Efforts during the period covered by this report were concentrated on *methods of cross-validation of the learning set to assess its internal* consistency. If the learning set fails to satisfy such tests for consistency, it is unlikely that extrapolation of discrimination results to new observations over areas of unknown favorability can be reliable. Therefore, satisfactory performance with respect to the procedure described below is a prerequisite for obtaining useful results using linear discriminant analysis.

Using single observations of counts and ratios, the Lubbock training set includes almost 7000 vectors of observations. As this is a large data set, and as adjacent observations cannot be considered statistically independent, we worked with a subset of about 700 observations. All of the independent variables (three spectral bands and their ratios) were included in the calculation of the discriminant function. No stepwise procedures were used.

Cross-validation is accomplished by splitting the learning set into two approximately equal subsets, A and B, calculating the linear discriminant function using A and using it to classify the observations in B. If the discriminant function correctly classifies about the same proportion of the second set B, which was <u>not</u> used in its computation, as of the first set A on which it was based, then the learning set is internally consistent.

The manner in which the learning set is split is important. Three methods are suggested here. First we may randomly split the "favorable" portion of the learning set into two subsets, A_F and B_F, and likewise split the "unfavorable" portion into A_U and B_U. A_F and A_U are then

used to estimate the linear discriminate function, and B_F and B_U are classified using the result. This random procedure fairly well guarantees that each of the original regions will be well represented in both the A and B subsets, and certainly consistency between these two subsets is a minimal requirement.

A more stringent procedure would be to divide each 100-record segment at its midpoint and assign one-half to the computational subset A, the other to the validation subset B. Using this procedure the observations which go into the computation of the linear discriminant function are at least somewhat separated, geographically, from those used for validation.

A third procedure is to split up the data by segments, randomly selecting half of the favorable segments and half of the unfavorable segments for the computational subsets and using all of the observations in these segments to estimate the discriminant function. The result is then tested using the remaining data from the other segments.

These three procedures were applied to the data in the Lubbock learning set, and the results are shown in Tables V, VI and VII. As is to be expected, the differences between the classification results for the "A" and "B" subsets are greatest for the third procedure, where whole segments are allocated to either the computational or the validation subset. Even in this case, however, the differences are not large.

TABLE V

Classification Results When the Learning Set is Divided Randomly

	Computational Set		Validation Set	
	correct	incorrect	correct	incorrect
Favorable	136. (76.4%)	42. (23.6%)	131. (76.2%)	41. (23.8%)
Unfavorable	156. (95.7%)	7. (4.3%)	161. (96.4%)	6. (3.6%)

TABLE VI

Classification Results When the Computational Set is Composed of One-half of Each Segment

	Computational Set		Validation Set	
	correct	incorrect	correct	incorrect
Favorable	132. (75.4%)	43. (24.6%)	137. (78.3%)	38. (21.7%)
Unfavorable	149. (90.3%)	16. (9.7%)	150. (90.9%)	15. (9.1%)

TABLE VII

Classification Results When the Learning Set is Divided by Segments

	Computational Set		Validation Set	
	correct	incorrect	correct	incorrect
Favorable	125. (74.0%)	44. (26.0%)	147. (82.1%)	32. (17.9%)
Unfavorable	144. (90.6%)	15. (9.4%)	146. (86.4%)	23. (13.6%)

By contrast, Tables VIII and IX give results obtained using the former method of basing the linear discriminant function on segment statistics. Since the statistics characterize whole segments, only the third of the procedures for splitting the data which were given above is applicable. It is clear that the model was overfitted in both cases, correctly classifying 97% to 100% of the computational subset but only 67% to 82% of the validation subset. Furthermore, there was almost no agreement between the two runs on which variables should be entered in the stepwise procedure. These results

TABLE VIII

Classification Results Using Sample Statistics Based on Segments (Computations using Set A)

	Computational Set		Validation Set	
	correct	incorrect	correct	incorrect
Favorable	15. (93.8%)	1. (6.3%)	14. (73.7%)	5. (26.3%)
Unfavorable	18. (100.0%)	0. (0.0%)	14. (93.3%)	1. (6.7%)

TABLE IX

Classification Results Using Sample Statistics Based on Segments (Computations using Set B)

	Computational Set		Validation Set	
	correct	incorrect	correct	incorrect
Favorable	19. (100.0%)	0. (0.0%)	10. (62.5%)	6. (37.5%)
Unfavorable	15. (100.0%)	0. (0.0%)	13. (72.2%)	5. (27.8%)

suggest that the discriminant functions computed in this way reflect only non-reproducible peculiarities of the data in the learning set and are not related to the favorability of the underlying areas.

Positive results obtained by using these cross-validation procedures do not guarantee that the resulting discriminant function will be useful, or that the numbers in a table such as Table VII are representative of the probabilities of correct classification of future observation. Good results may simply indicate that the learning set was narrowly restricted and not truly representative of the area of interest. However, poor results would strongly suggest that subsequent classification of new observations would be almost worthless.

Note: It was mentioned in Ref. 9 that among the assumptions underlying linear discriminant analysis (or at least the estimation of the "posterior probability" of favorability) is an assumption of multivariate normality. Normal and lognormal distributions were fit to each segment of 100 records in the Lubbock learning set. Neither distribution appeared to provide a superior fit, and in particular there seems to be no reason to reject the hypothesis of normality, or to transform the data prior to performing the analysis.

IV. LANDSAT DATA BASE

LANDSAT data was obtained for a portion of the Lubbock quadrangle. During the period covered by this report a subset of this data corresponding to the flight lines flown during the aerial survey was extracted.

First the size of the data base (originally unmanageably large, and in any case representing greater resolution than that obtained by the aircraft flying 400 feet above the ground) was reduced by averaging over rectangles of 3 x 4 observations ("pixels"). This resulted in a map of about 250,000 points (with observations in four spectral bands at each point) covering approximately the western half of the Lubbock quadrangle.

The rectangular grid on which the LANDSAT data is collected as the satellite passes overhead is skewed with respect to normal mapping grids and does not correspond to any standard map projection. The LANDSAT coordinate system was modeled as a quadratic transformation of longitude and latitude

$$\begin{pmatrix} \xi \\ \eta \end{pmatrix} = \begin{pmatrix} a_1 \\ b_1 \end{pmatrix} + \begin{pmatrix} a_2 & a_3 & a_4 & a_5 & a_6 \\ b_2 & b_3 & b_4 & b_5 & b_6 \end{pmatrix} \begin{pmatrix} \lambda \\ \phi \\ \lambda^2 \\ \lambda\phi \\ \phi^2 \end{pmatrix}$$

where (ξ, η) are the LANDSAT coordinates of a point with longitude λ, latitude ϕ. The parameters of this model were fitted by least squares, using 11 points in the Lubbock area which could be identified in the LANDSAT pictures and whose latitude and longitude were known.

The radiometric data are available at 300 points along each of 23 flight lines. The latitude and longitude of each of these points was obtained by

table look-up and transformed to LANDSAT coordinates by Eq. (1). The corresponding LANDSAT values in each spectral band were obtained by bilinear interpolation from the nearest grid points. (See Fig. 10.)

Pictures of the resulting data base are shown in Fig. 11.

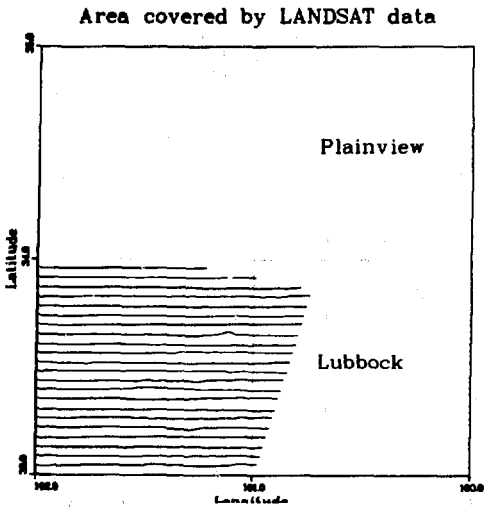

Fig. 10. Area covered by LANDSAT data.

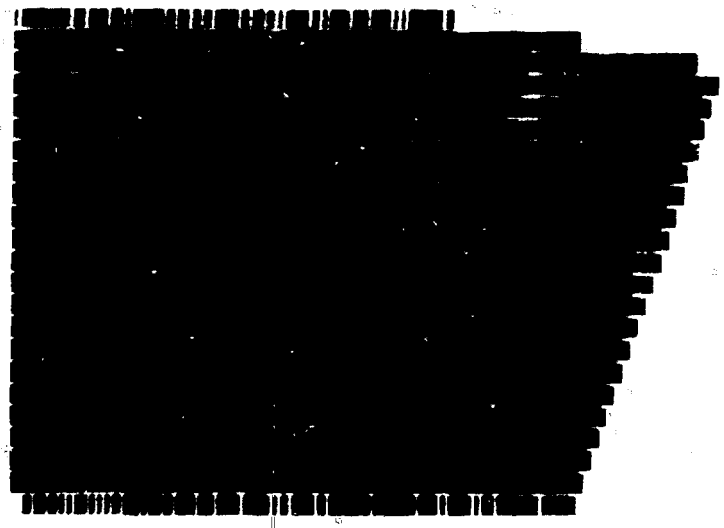

Fig. 11a. LANDSAT data in western part of Lubbock quadrangle--Band 1.

Fig. 11b. LANDSAT data in western part of Lubbock quadrangle--Band 2.

Fig. 11c. LANDSAT data in western part of Lubbock quadrangle--Band 3.

Fig. 11d. LANDSAT data in western part of Lubbock quadrangle--Band 4.

V. BIAS AND RATIOS

During the period covered by this report we continued our investigation of the observational bias suggested in Ref. 10. If the aerial radiometric data can be modeled as the output of a linear system, then the observations at coordinates (x_0,y_0) are given by an integral of the form

$$S_i(x_0,y_0) = \iiint s(x,y,E)r_i(x_0-x,y_0-y,E)dxdydE + \varepsilon_i \ , \qquad (1)$$

where $s(x,y,E)$ is the energy spectrum associated with a ground point (x,y) and $r_i(\xi,\eta,E)$ is the response of the detector in the ith band to energy at frequency E located at (ξ,η) relative to the detector. ε_i is an error term. (The altitude of the detector is taken to be constant, so that this model involves only two spatial dimensions.)

Now suppose the spectrum $s(x,y,E)$ is the product of a term characteristic of the underlying geological type, $S_G(E)$, and a spatially varying intensity function, $k_1(x,y)$. (This appears to be the model behind the idea that the ratio of two bands may be more stable than observations in either band.) Suppose also that the system response function is separable, that is, $r_i(\xi,\eta,E) = p(\xi,\eta)h_i(E)$. Then the observations S_i will be of the form

$$S_i(x_0,y_0) = K(x_0,y_0) \cdot H_i(G) + \varepsilon_i \qquad (2)$$

where

$$K(x_0,y_0) = \iint k_1(x,y)p(x_0-x,y_0-y)dxdy$$

and

$$H_i(G) = \int h_i(E)S_g(E)dE.$$

Under the model Eq. (2), therefore, the observations over a homogeneous geological region G should cluster around a line in the direction of the vector $(H_1(G),\ldots H_b(G))$ (where b bands are observed), passing through the

origin. The ratios $S_i(x_0,y_0)/S_j(x_0,y_0)$ should be quite stable unless the assumption that

$$S(x,y,E) = k(x,y)S_G(E)$$

fails. This may occur as the result of leaching or concentration of certain elements which would distort the normal spectral relationship.

On the other hand, if there is some background radiation or other form of bias in the observation process, Eq. (2) becomes

$$S_i'(x_0,y_0) = K(x_0,y_0)H_i(G) + B_i + \varepsilon_i, \tag{3}$$

and the ratios S_i'/S_j' are no longer approximately independent of (x_0,y_0). However, the ratios

$$\frac{S_i'(x_0,y_0) - B_i}{S_j'(x_0,y_0) - B_j}$$

continue to have the useful properties described above and therefore it might be of interest to see if the B_i can be estimated and if they appear to be different from zero.

As explained in Ref. 10, this can be done by estimating the best line fitting the data for each geological type (which is the first principal component for these data) and then estimating the point at which these lines come closest to intersecting. This point was estimated to be

Th = 44.60
Bi = 71.38
K = 166.85,

and Table X gives the distances from the best fitting lines to this point, as well as to the origin, for each geological type considered. On the basis of this table it seems that the lines come significantly closer to intersecting at the point given above than at the origin.

TABLE X

Comparison of the Distances of the Principal Component Vectors from Two Points

GEOLOGICAL TYPE	NUMBER OF POINTS IN SAMPLE	DISTANCE FROM ORIGIN	DISTANCE FROM 'INTERSECTION'
PSA	(54)	42.13	16.11
PB	(1727)	46.25	8.02
PWH	(2273)	46.97	6.28
PQ	(1269)	52.03	8.48
TRD	(979)	105.88	8.07
TO	(885)	177.35	7.07
QCS	(4263)	14.05	10.39
QP	(198)	12.37	13.07
QT	(370)	11.17	7.63
QS	(1290)	3.54	23.86
QSD	(91)	14.96	6.03
QAL	(329)	40.66	6.20

However, the plot in Fig. 12 casts some doubt on this conclusion. From this plot it seems clear that the two formations To and Trd have first principal components which deviate significantly from the others, and it appears to be these which are pulling the "intersection" away from the origin. These formations are known to have a number of outliers, which affect the estimate of the first principal component disproportionately, much as they do the estimates of mean and variance. Therefore this computation will be repeated with a more robust estimation technique.

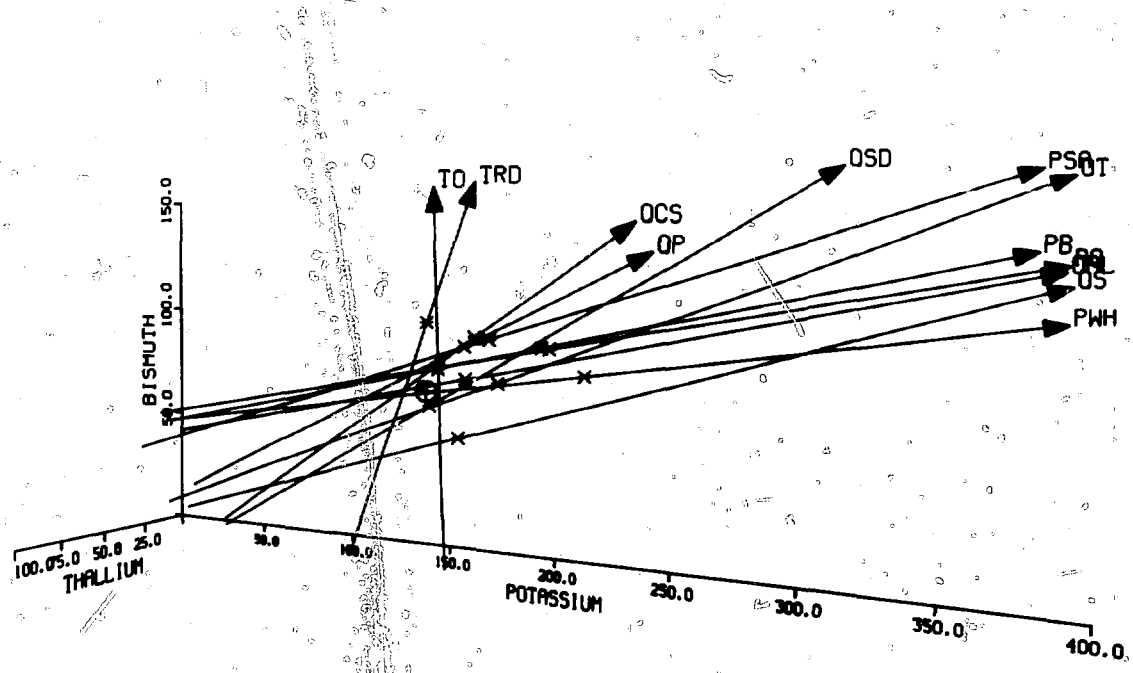

Fig. 12. First principal component vectors for twelve geological formations.

REFERENCES

1. G. W. Wecksung, K. Campbell, and T. R. Bement, "Computer Graphics and the Analysis of National Uranium Resource Evaluation Data," presented at the Fall Convention of the American Congress on Surveying and Mapping and the American Society of Photogrammetry, Albuquerque, NM, October 29, 1978.

2. F. L. Pirkle, K. Campbell, and G. W. Wecksung, "Principal Component Analysis as a Tool for Interpreting NURE Aerial Radiometric Survey Data," submitted to the Journal of Geology.

3. T. R. Bement, D. V. Susco, D. E. Whiteman, and R. K. Zeigler, "Geostatistics Project of the National Uranium Resource Evaluation Program, January-March 1977," Los Alamos Scientific Laboratory report LA-6804-PR.

4. T. R. Bement and M. S. Waterman, "Locating Maximum Variance Segments in Sequential Data," Mathematical Geology 9, No. 1 (1977), pp. 55-61.

5. T. R. Bement, K. Campbell, G. W. Wecksung, M. D. McKay, and R. K. Zeigler, "Geostatistics Project of the National Uranium Resource Evaluation Program, January-March 1978," Los Alamos Scientific Laboratory report LA-7296-PR.

6. K. Campbell, G. W. Wecksung, D. E. Whiteman, and T. R. Bement, "Geostatistics Project of the National Uranium Resource Evaluation Program, April-June 1978," Los Alamos Scientific Laboratory report LA-7463-PR.

7. R. K. Zeigler, D. V. Susco, G. W. Wecksung, K. Campbell, and T. R. Bement, "Geostatistics Project of the National Uranium Resource Evaluation Program, April-June 1977," Los Alamos Scientific Laboratory report LA-6935-PR.

8. "Study of Airborne Gamma-ray Spectrometer Data Procedures, Wind River Basin, Wyoming: Final Report," Texas Instruments Incorporated, January, 1979.

9. T. R. Bement and D. E. Whiteman, "Geostatistics Project of the National Uranium Resource Evaluation Program, July-September 1978," Los Alamos Scientific Laboratory report LA-7608-PR.

10. T. R. Bement, M. D. McKay, and G. W. Wecksung, "Geostatistics Project of the National Uranium Resource Evaluation Program, October-December 1977," Los Alamos Scientific Laboratory report LA-7168-PR.